Dilution-Induced Hierarchical Self-Assembly of nanovesicles: the Role of Hydrophobic Hydration

Dapeng Liu, Xiaosong Wang

Department of Chemistry and Waterloo Institute for Nanotechnology (WIN), University of Waterloo, 200 University Ave, Waterloo, ON, Canada N2L 3G1.

Introduction

Hydrophobic Hydration (HH) functions inevitably in the solution behaviour of biological assemblies, such as dilution-induced refolding of denatured proteins. Although HH, sensitive to subtle changes in solution conditions, is being studied via simulation and characterization of hydrated water, the solution behaviour of solutes in response to HH is difficult to study without appropriate model systems. Amphiphiles are commonly used for aqueous assemblies, in which the role of HH is concealed by a strong affiliation of water with water-soluble heads. Systems with colloidal behaviour sensitive to HH, therefore, are desirable to enable this investigation.
Herein, we report that the relative HH level of Fe[δ^+] and O[δ^-] in Fp$(CH_2)_6$Azobenzene^{trans} (*trans*: trans configuration) MCsomes can be adjusted by the concentration, which is confirmed by electrochemical, fluorescence (FL) quenching experiments, and zeta potential measurement. The variation in HH, induced by dilution, initiated the self-assembly of the MCsomes into helical structures (Figure 1). This study firstly reveals the role of HH in dilution-induced self-assemblies in water. In addition, unlike many reported assemblies of solid nanoparticles, this system provides an opportunity to understand the structural evolution of vesicles.

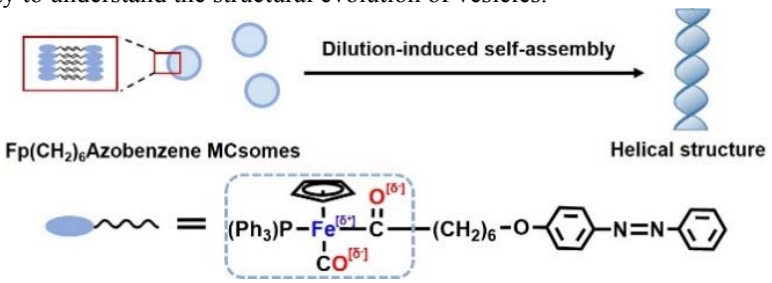

Figure 1. Schematic illustration of the dilution-induced self-assembly from Fp$(CH_2)_6$Azobenzene^{trans} Mcsomes into helical structure in water.

Results and discussion

Dilution-induced self-assembly of Fp$(CH_2)_6$Azobenzenetrans nanovesicles

Fp$(CH_2)_6$Azobenzene^{trans} molecules are hydrophobic and non-surface active and can self-assemble in water using THF as a common solvent. And Fp$(CH_2)_6$Azobenzene^{trans} assembles into MCsomes (140 μM) (Figure 2a) with detectable WCIs. The zeta potential (ζ) of the colloids is *ca.* -51 ± 0.8 mV, suggesting that the HH of O[δ^-], relative to Fe[δ^+], is stronger due to the presence of WCIs. The size of the nanovesicles is *ca*. 168 nm (Figure 2a) and remains unchanged after aging for 25 days (Figure 2b). However, the time-resolved DLS indicates that the diluted MCsomes (14 μM), unlike those at 140 μM, enlarges to micrometres over 25 days (Figure 2b). The TEM image of the aged sample shows a helical morphology (Figure 2c) that is supported by the Electron energy loss spectrum (EELS) of C elements. As shown in Figure 2d, the distribution of C elements is wave-shaped along the helix and is higher in the middle when the cross section is analysed. The helical pitch is *ca.* 500 nm, the width is *ca.* 500 nm (Figure 2c).

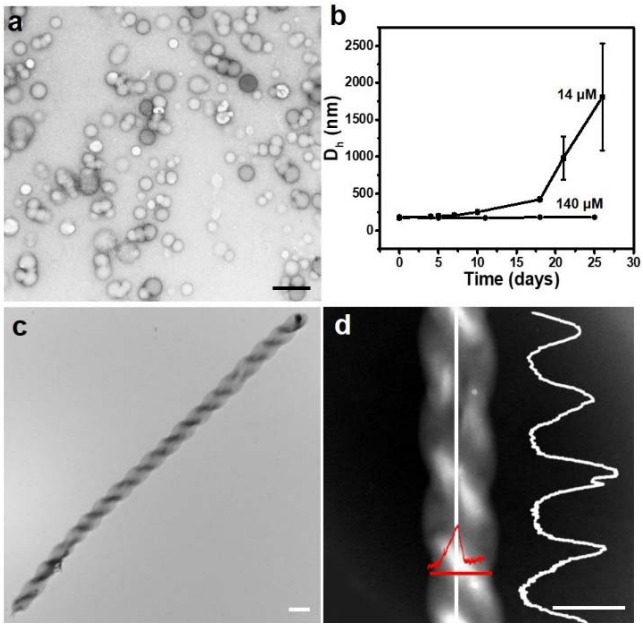

Figure 2. (a) TEM image of the MCsome assembled from $Fp(CH_2)_6Azobenzene^{trans}$ in water (140 μM). (b) The time-resolved D_h of $Fp(CH_2)_6Azobenzene^{trans}$ MCsomes in water for the solutions with concentrations of 140 μM and 14 μM. (c) TEM image of the helix assembled from $Fp(CH_2)_6Azobenzene^{trans}$ MCsomes that were diluted to 14 μM and aged for 30 days. (d) Electron energy loss spectrum (EELS) of carbon elements distributing along and normal to the helical axis. Scale bar: 500 nm.

The conditional effect of HH.

HH is a conditional effect depending on the solution conditions. This elusive concept was examined using MCsomes as a model system (Figure 3a). As shown in Figure 3b, the dilution reduces the net surface charge. This was because that the HH of $Fe[\delta^+]$ is enhanced upon the dilution. This enhancement is confirmed by cyclic voltammetry (CV) experiments. As shown in Figure 3c, the oxidation signals due to the hydrated $Fe[\delta^+]$ at 140 μM are barely detectable, but appears even after 10 times dilution to 14 μM. In addition, the oxidation coupling ($\Delta E_{½}$) of the two-oxidation peaks is smaller for the solution with a lower concentration, suggesting that the distance between the Fp heads ($d_{Fp\text{-}Fp}$) in close proximity is increased, resulting from the dilution-enhanced HH. This concentration-dependent hydration of $Fe[\delta^+]$ is further verified by fluorescence (FL) quenching experiments. Figure 3d shows that the Stern-Volmer plot for the solution of calcein is a downward curve as the MCsomes is diluted, because the dilution-enhanced HH of $Fe[\delta^+]$ facilitates its interaction with the water-soluble dye and enhances the quenching effect. To show that the ζ results from the charge balance between the hydrated $Fe[\delta^+]$ and $O[\delta^-]$, the pH-dependent ζ was measured. As shown in Figure 3e, the ζ of MCsomes at 140 μM reduces to *ca.* -26 mV by lowering the pH to 3.0 due to the protonation of $O[\delta^-]$. For the diluted solution (14 μM), the ζ at pH 3 is even lower (ca. -8.2 mV) due to the combined effect of protonation of $O[\delta^-]$ and dilution-enhanced HH of $Fe[\delta^+]$ (Figure 3a).

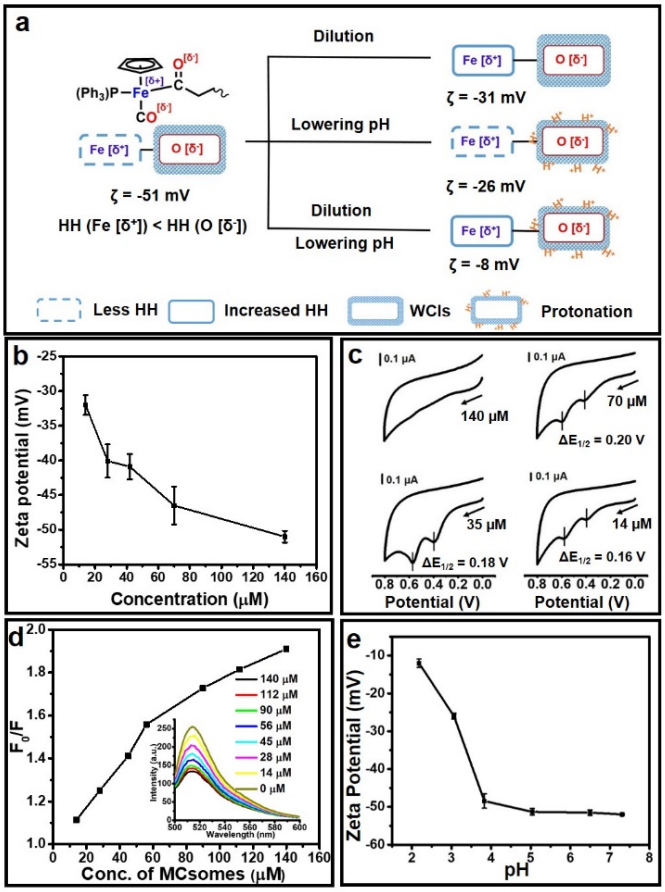

Figure 3. (a) Schematic illustration for the hydrophobic hydration (HH) of Fp head in response to dilution and lowering pH. The zeta potential of the $Fp(CH_2)_6Azobenzene^{trans}$ MCsomes in dependence of the dilution from 140 μM to 14 μM and pH lowering from 7.3 to 3.0 is indicated in the scheme. (b) Zeta potential of $Fp(CH_2)_6Azobenzene^{trans}$ MCsome in water in response to dilution process (from 140 μM to 14 μM). (c) The cyclic voltammogram (CV) for $Fp(CH_2)_6Azobenzene^{trans}$ MCsome in water with the concentration of 140 μM, 70 μM, 35 μM and 14 μM, respectively. (d) The Stern-Volmer plot for the fluorescence quenching of calcein (0.17 μM) in water by $Fp(CH_2)_6Azobenzene^{trans}$ MCsomes with different concentrations. The inset displays the corresponding emission spectra. F_0 and F refer to the emission intensity of calcein in the absence and presence of MCsomes. (e) pH-dependent zeta potential of $Fp(CH_2)_6Azobenzene^{trans}$ MCsome in water (140 μM).

Hierarchical self-assembling behaviour.

The dilution trigged a hierarchical self-assembly, which is caused by the suppression of coulombic repulsions due to the dilution-enhanced HH of Fe[δ^+] (Figure 3). The TEM images were recorded at different stages of the assembly. As shown in Figure 4a and 4b, the diluted MCsomes (14 μM) fuse and enlarge from *ca.* 170 nm to *ca.* 500 nm in diameter after aging for *ca.* 10 days to lower the membrane tension and the interfacial energy. Several intermediates at different fusion stages, including hemifusion and full fusion, are shown in Figure 4c. On the day 14 of the assembly process, one-dimensional arrays of vesicles are observed (Figure 4d). This behaviour is attributed to the dipole-dipole interactions of the dielectric MCsomes that possess a local electric field. The majority of the vesicles in the arrays are of larger size (*ca.* 500 nm in diameter) (Figure 4d), indicating that the fusion occurs prior to the one-dimensional assembly. Upon aggregation, the vesicular membrane starts to coalesce (Figure 4e) and the arrays evolve into nanotubes (Figure 4f) as indicated by the TEM images taken at day 20. The parallel packing of aromatic groups may result in the formation of nanotube with lower curvature. These nanotubes eventually evolve into helixes, which is attributed to the packing behaviour of asymmetric *trans*-azobenzene groups (Figure 4g). This nanotube-to-helix transition is supported by the intermediate as shown in Figure 4h, in which the assembly is partially twisted. The tube-to-helix transition was reported before for lipid bilayer membranes.

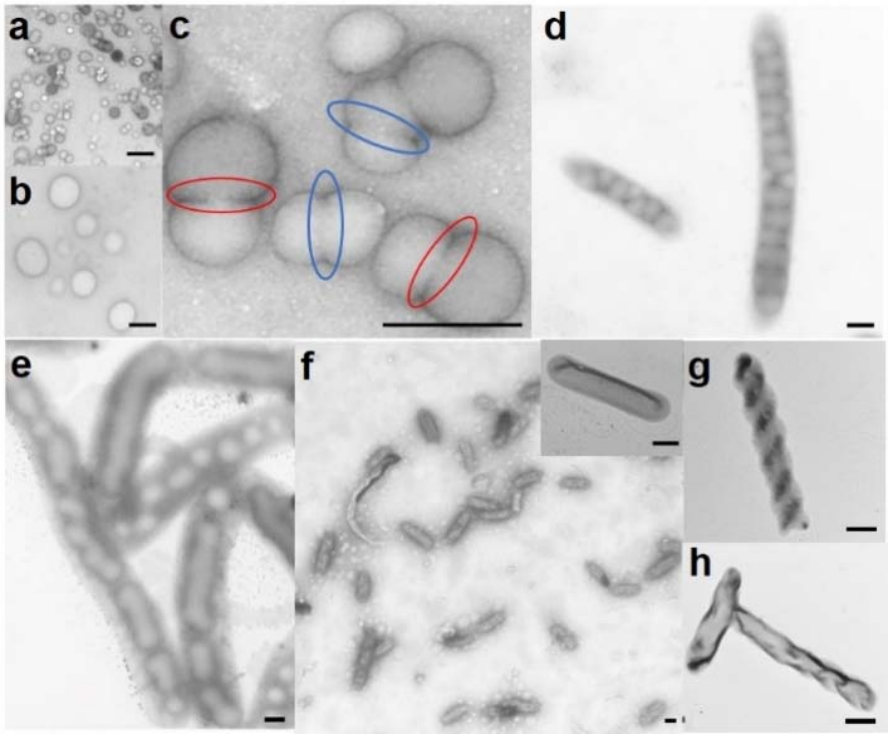

Figure 4. (a-h) TEM images for the diluted $Fp(CH_2)_6Azobenzene^{trans}$ MCsome (14 μM) in water at different aging times. (a) Initially prepared MCsomes, (b) Fused MCsomes after aging for 10 days, (c) Fusion intermediates. The red circles represent hemifusion where the thickness of the contact zone is close to the membrane thickness and the blue circles represent full fusion where two vesicles are fused without membrane separation, (d) One-dimensional arrays of vesicles after aging for 14 days, (e) Intermediates for the coalescence of the vesicles into nanotubes, (f) Hollow tube structures after aging for 20 day, (g) Helical structures after aging for 30 day, (h) The intermediates for tube-to-helix transition.

Conclusion

The role of HH effect on self-assembly was studied using $Fp(CH_2)_6Azobenzene^{trans}$ MCsomes. The highly polarized Fp head (with Fe-CO groups) in the MCsomes contains hydrated $O[\delta^-]$ via WCIs and less hydrated $Fe[\delta^+]$. By taking advantage of the detectable hydration of $Fe[\delta^+]$, we elucidated the conditional HH effect and explicated how this effect trigged an assembly of MCsomes. The subsequent hierarchical self-assemblies of MCsomes generated high-level structures. This evolution was explained based on the understanding of electrostatic, dipole-dipole, π-π interactions, etc. This study using the molecular model system, complementary to the research focusing on hydrated water, is essential to evaluate and create the theory of HH for an improved understanding of biological events and rational design of waterborne materials.